Nanometric Thin Skinned Dual-Layer Hollow Fiber Membranes for Dehydration of Isopropanol

Yu Pan Tang
NUS Graduate School for Integrative Sciences and Engineering, National University of Singapore, 28 Medical Drive, Singapore 117456

Dept. of Chemical and Biomolecular Engineering, National University of Singapore, 4 Engineering Drive 4, Singapore 117576

Natalia Widjojo
BASF South East Asia Pte Ltd, A-GMM/F, 61 Science Park Road #03-01, Singapore 117525

Tai Shung Chung
NUS Graduate School for Integrative Sciences and Engineering, National University of Singapore, 28 Medical Drive, Singapore 117456

Dept. of Chemical and Biomolecular Engineering, National University of Singapore, 4 Engineering Drive 4, Singapore 117576

Martin Weber
Performance Materials, BASF SE, GMV/W-B1, 67056 Ludwigshafen, Germany

Christian Maletzko
Engineering Plastics, BASF SE, E-KTE/NE-F206, 67056 Ludwigshafen, Germany

DOI 10.1002/aic.14067
Published online March 13, 2013 in Wiley Online Library (wileyonlinelibrary.com)

A novel sulfonated polyphenylsulfone (sPPSU)/polyphenylsulfone (PPSU)-based dual-layer hollow fiber membrane with a nanometric thin skin layer has been designed for biofuel dehydration via pervaporation. The thickness of skin selective layer is in the range of 15–90 nm under different spinning conditions measured by positron annihilation spectroscopy (PAS) coupled with a mono-energetic positron beam. The effects of outer-layer dope properties, coagulation temperature, and dope flow rate during spinning were systematically investigated. By tuning these spinning parameters, a high performance sPPSU/PPSU-based dual-layer hollow fiber membrane with desirable morphology was successfully obtained. Particularly owing to its nanometric thin skin layer, a high flux of 3.47 kg/m^{2}h with a separation factor of 156 was achieved for dehydration of an 85 wt % isopropanol aqueous solution at 50°C. After post thermal treatment at 150°C for 2 h, the separation factor was dramatically improved to 687 while flux dropped to 2.30 kg/m^{2}h, which make it comparable to the inorganic membranes. In addition, excellent correlations were found among the results from field emission scanning electron microscopy, PAS spectra, and separation performance. © 2013 American Institute of Chemical Engineers *AIChE J*, 59: 2943–2956, 2013

Keywords: pervaporation, isopropanol dehydration, dual-layer hollow fiber membrane, positron annihilation spectroscopy

Introduction

Pervaporation, a fast-growing membrane-based separation technique, has been extensively studied due to its distinctive features such as (1) low capital and operation cost, (2) high energy efficiency, (3) simple operation and small footprint, (4) multipurpose applications and easy scale-up, and (5) ability to separate azeotropic mixtures and close-boiling point mixtures.[1,2] In our previous work,[3] dense flat membranes fabricated from direct sulfonated polyphenylsulfone (sPPSU) polymers with different degrees of sulfonation were applied to dehydrate C1—C4 alcohols via pervaporation. The sPPSU polymers were originally selected due to their following characteristics: (1) comprising rigid polymer chains that possess high mechanical and hydrothermal stability; (2) containing sulfonate groups that facilitate water transport across membranes; and (3) possessing suitable d-spacing that enables to separate water from organics. Partially consistent with our hypotheses, the dense flat membranes demonstrated the potential of sPPSU for dehydration of C1—C4 alcohols

Correspondence concerning this article should be addressed to T.S. Chung at chencts@nus.edu.sg.

with high separation factors but disappointed productivity (i.e., low flux or permeability). The unimpressive permeation flux is an inevitable obstacle for further commercialization.

Several approaches have been used to improve membranes' permeation flux, namely, (1) fabricating anisotropic membranes to reduce the dense-selective layer thickness, (2) increasing the free volume of selective layer materials (i.e., polymer blends[4–6] and mixed matrix membranes with inorganic fillers[7–11]), and (3) elevating the operating temperature to facilitate the thermal motion of polymer chains. Fabrication of anisotropic membranes (i.e., asymmetric or composite membrane) is the most commonly used method to largely increase the permeation flux. In general, an asymmetric membrane contains an integrally skinned selective layer and a porous support layer, whereas a composite membrane consists of a selective layer and a porous substrate made from different materials. The composite membrane may be more attractive due to the synergism of potentially combining the strengths of different materials. Composite membranes are typically prepared by coating,[12] layer-by-layer assembly (LBL),[13–16] interfacial polymerization (IP),[17–19] or plasma polymerization[20,21] of the dense selective layer on top of the substrate.

Compared to flat-sheet membranes, the development of hollow fiber membranes for pervaporation is more practical because hollow fibers offer the advantages of high packing density, mechanically self-supporting structure, and relatively low cost.[1,2] Particularly in the recent years, the superiority of dual-layer over single-layer hollow fiber membranes has been fully demonstrated. By using one-step co-extrusion process, the dual-layer hollow fiber synergistically combines the strengths of both single-layer hollow fiber and composite membrane. Not only does it have the unique capability to exploit expensive and high-performance materials as the selective layer, but also substantially reduce the substructure resistance by using another material or less concentrated polymer solution as the inner layer. As a result, the problem of solvent-induced swelling in the substrate can be significantly mitigated by choosing a substrate material with superior chemical resistance. However, the development of polymeric dual-layer hollow fiber membranes for pervaporation is still far behind the flat-sheet membranes due to the complicated controlling parameters during spinning. It is always challenging to form dual-layer hollow fibers with an ultrathin defect-free skin layer, and it is also hard to molecularly design the dense-selective layer with minimal solvent-induced swelling. In addition, concentration polarization in fine hollow fibers and delamination between the inner and outer layers often occur limiting the pervaporation performance.

To overcome the aforementioned deficiencies for pervaporation, dual-layer hollow fiber membranes fabricated from a variety of polymer materials have been studied in our lab[22–27] with different engineering and design parameters during spinning and post modifications. Liu et al.[22] investigated the effects of air gap distance and dope flow rate on the morphology and pervaporation performance of P84 co-polyimide/polyethersulfone dual-layer hollow fiber membranes. The as-spun fibers had a flux up to 1.5 kg/m^{2}h with a separation factor less than 100 for dehydration of isopropanol (IPA). After post treatments by *p*-xylenediamine crosslinking and thermal annealing, the resultant fibers achieved a high separation factor of 953, but reduced the original flux to one half. Polybenzimidazole/P84 dual-layer hollow fiber membranes were also applied to pervaporatively dehydrate tetrafluoropropanol and acetone by Wang et al.[23] and Shi et al.,[24] respectively. A permeation flux of 0.3 kg/m^{2}h with a separation factor of 1990 were achieved for dehydration of tetrafluoropropanol without any post treatment. While, a much lower separation performance was obtained for dehydration of acetone even after both chemical crosslinking and heat modification since acetone dehydration is particularly challenging. In addition, an inspiring study by Jiang et al.[25] revealed that an ultrathin dense selective layer could be formed at the interface of the inner- and outer-layer materials (Udel® Polysulfone and Matrimid® 5218) due to the formation of an interpenetration network. Their membranes had an impressive flux of 2.56 kg/m^{2}h and a good separation factor of 1100 for dehydration of an 86 wt % tert-butanol aqueous solution at 80°C. Recently, Wang et al.[26] and Widjojo et al.[27] conducted systematic studies on alcohols dehydration using dual-layer hollow fiber membranes made of polyamide-imide and polyimide as selective layers, respectively. Their membranes showed high separation factors (>1000) with moderate fluxes for dehydration of IPA and butanol.

Nevertheless, except limited cases, most polymeric dual-layer hollow fiber membranes cannot compete with inorganic membranes[28–32] due to the inherently relatively low separation performance (either flux or separation factor) of polymers. Additionally, the formation of an ultrathin skin layer on hollow fiber membranes is the key factor to achieve high productivity, but it is not a trivial task. To break the deadlock, the objectives of this work are (1) to elucidate the fundamental science on how to molecularly design dual-layer hollow fiber membranes with a nanometric thin skin layer for IPA dehydration and (2) to identify key processing factors for the fabrication of dual-layer hollow fiber membranes with high productivity and separation efficiency. Polyphenylsulfone (PPSU) and sPPSU polymers were chosen as the inner- and outer-layer materials, respectively, because PPSU possesses outstanding antiswelling property and sPPSU shows a high intrinsic selectivity for IPA dehydration. Concurrently, a 50/50 (wt/wt) sPPSU/PPSU blend was also explored as the outer-layer materials to enhance its antiswelling property. In addition, correlations among the results from field emission scanning electron microscopy (FESEM), positron annihilation spectroscopy (PAS), and separation performance were systematically studied to discover fundamentals to design better pervaporation membranes for the years to come.

Experimental

Materials

Both sPPSU and PPSU polymers were supplied by BASF SE, Germany. The sPPSU polymer was synthesized by using the directly copolymerized sulfonation method with 1.5 mol % 3,3′-disulfonate-4,4′-dichlorodiphenyl sulfone monomer. Figure 1 shows their chemical structures. An analytical grade *N*-Methyl pyrrolidone (NMP) was supplied by Merck and used as received as the solvent. IPA purchased from Fisher Scientific was used to prepare binary aqueous feed solutions with a water concentration of 15 wt %. IPA has been extensively used in pharmaceutical and electronic industries and its recycle has received worldwide attention. IPA forms an azeotrope with water at 88 wt %,[33] and this makes it difficult to be separated from water by conventional processes.

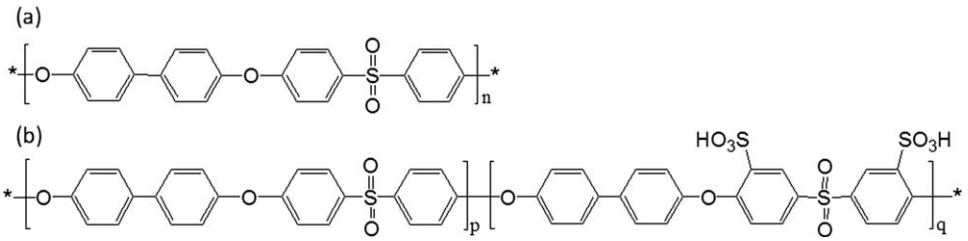

Figure 1. Chemical structures of: (a) PPSU (nonsulfonated); (b) sPPSU (p = 98.5 mol %; q = 1.5 mol %).

Dope preparation and viscosity measurements

Homogeneous dope solutions were prepared by fully dissolving desired amount of polymers in NMP with the aid of a Eurostar power-control stirrer. Viscosities of both PPSU and sPPSU polymers were measured as a function of polymer concentration to identify suitable outer-layer dope concentrations for spinning. An ARES Rheometric Scientific rheometer with a 25-mm cone plate was used for viscosity measurements at ambient temperature in a shear rate range of 1–100 s^{-1}. Figure 2 shows the dope viscosity at the shear rate of 10 s^{-1} vs. polymer concentration in NMP. A power-law fluid model was applied to fit the rheological data and to express the relationship between shear stress $\tau(N/m^2)$ and shear rate $\gamma(s^{-1})$ as follows

$$\tau = K|\gamma|^n \tag{1}$$

Eq. 1 is assumed to be applicable to describe the rheological behavior of polymer solutions within the spinnerets during spinning. Table 1 tabulates their empirical power law equations and indicates that PPSU has a lower viscosity and behaves more like a Newtonian fluid than sPPSU. The critical polymer concentrations, determined by the intersection of two slopes as illustrated in Figure 2, are 29.3 and 30.2 wt % for PPSU and sPPSU dopes, respectively.

Fabrication of dual-layer hollow fiber membranes

The dual-layer hollow fiber membranes were fabricated by the co-extrusion technique using a triple-orifice spinneret. The spinning procedure had been described elsewhere.[22–27] After being fully degassed, the outer and inner polymer dopes were loaded into two syringe pumps (ISCO 1000), followed by further overnight degassing. A mixture of 95/5 (w/w) NMP/water was used as the bore fluid to slow down phase inversion and produce a porous inner surface. Polymer dopes and bore fluid were filtered through sintered metal filters of 15 μm in pore size when being extruded out of the ISCO syringe pumps at ambient temperature. Tap water was used as the external coagulant. Table 2 summarizes the detailed spinning conditions for the dual-layer co-extrusion process, whereas Table 3 gives their identification number (ID) and their corresponding preparation conditions. The as-spun hollow fibers were stored in water for three days to remove residual solvents, followed by solvent-exchange in methanol and hexane three times and each for 30 min. Subsequently, they were dried in air naturally.

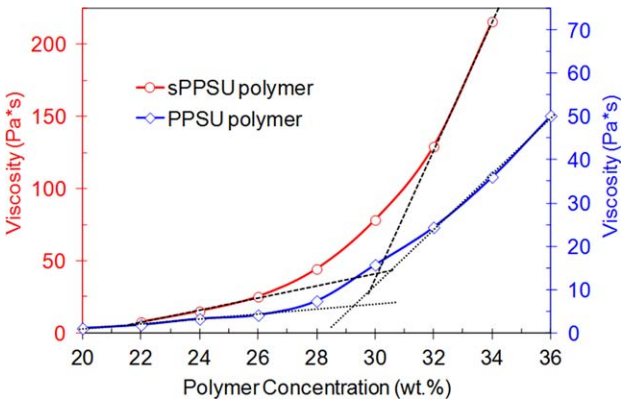

Figure 2. Viscosity of sPPSU and PPSU polymers as a function of polymer concentration (Shear rate:10 s^{-1}; Solvent: *N*-Methyl-2-pyrrolidone).

[Color figure can be viewed in the online issue, which is available at wileyonlinelibrary.com.]

Characterizations

Field Emission Scanning Electronic Microscopy (FESEM). The morphology of dual-layer hollow fiber membranes was observed by a field emission scanning electron microscope (FESEM JEOL JSM-6700F). Before observation, the hollow fibers were immersed in liquid nitrogen, fractured, and then coated with platinum using a JEOL JFC-1300 Platinum coater.

Positron Annihilation Spectroscopy. PAS,[34–36] as a relatively new technique, has been proved to be a powerful tool for both qualitative and quantitative examination of local free volume properties at the atomic scale (i.e., 1–10 Å) in polymers. By using mono-energetic positron beams, PAS is able to study the morphologies and depth profiles of the surface or near surface of an asymmetric polymeric membrane.[25,35] Several types of positron experiments have been developed in polymers using a positron beam, namely, positron annihilation lifetime spectroscopy (PALS), doppler broadening energy spectroscopy (DBES), aged momentum correlation, and angular correlation of annihilation radiation. PALS and DBES are the two most frequently used methods to characterize pore sizes in membranes. The usefulness of PAS for characterizing polymeric membranes has been iteratively demonstrated in recent works.[17–19,25,35,37,38]

The dual-layer hollow fiber membranes were measured by DBES using PAS coupled with a slow positron beam in our

Table 1. Power Law Equations for the Polymer Dope Solutions

Polymer composition (wt/wt)	Polymer concentration (wt%)	$\tau = K\|\gamma\|^n$	
		K	n
sPPSU	32	142.7	0.9242
sPPSU/PPSU (50/50)	32	113.9	0.9114
PPSU	32	24.6	0.9410

Table 2. Spinning Parameters of sPPSU/PPSU Based Dual-Layer Hollow Fiber Membranes (Inset Shows the Spinneret Dimensions). [Color table can be viewed in the online issue, which is available at wileyonlinelibrary.com.]

Spinning parameter		Condition			
Dope composition - (wt%)	Inner layer		20/15/65 (PPSU/EG/NMP)		
	Outer layer	15/15/70 (sPPSU/PPSU/NMP)	16/16/68 (sPPSU/PPSU/NMP)	32/68 (PPSU/NMP)	32/68 (sPPSU/NMP)
Bore fluid composition (wt%)			95/5(NMP/water)	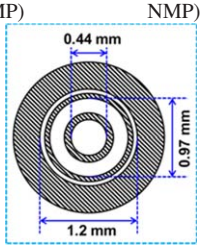	
Bore flow rate (ml/min)			1.5		
Spinneret dimension (mm)			1.2/0.97/0.44		
Air gap length (mm)			10		
External coagulant			Tap water		
Spinning temperature			Ambient temperature(AT)		
Coagulation temperature		Ambient temperature	Ambient temperature and 10°C	10°C	10°C
Dope flow rate (ml/min)	Inner layer		2		
	Outer layer	0.1	0.1/0.2/0.3/0.5/0.7	0.1	0.1
Take up speed (m/min)			Free fall		

A radioisotope ^{22}Na with energy of 50 mCi was used as the positron source. The positrons emitted from the source were moderated in a tungsten mesh and filtered through an E × B filter. After filtration, the slow positrons were accelerated at a variable mono-energy (from 0.1 to 30 keV), then magnetically focused towards the sample chamber and finally hit on the sample. The samples were prepared by sticking hollow fibers in parallel on an aluminum plate holder to form a square surface with the area about 2.5 × 2.5 cm^2. Two layers of fiber were packed to form a seamless surface. The DBES spectra were recorded using an HP Ge detector at a counting rate of approximately 1000 cps and the total number of counts for each spectrum was 1.0 million. The mean depth Z of the polymeric materials where the positron annihilation occurs is calculated from E_+ by using the following equation[35,36]

$$Z(E_+) = \left(\frac{40}{\rho}\right) \times E_+^{1.6} \tag{2}$$

where Z is the depth in nm, ρ is the material density in g/cm^3, and E_+ is the incident positron energy in keV. This equation was mostly applied to calculate the mean depth for membranes with a planar geometry. Since there is currently no suitable equation for cylindrical geometry, we have applied this equation in this work to estimate the depth from incident energy. When we fitted the R curves using VEPFIT software, the polymer density was used as the density of the dense skin layer, whereas the density was progressively reduced by 0.3 for the transition layer and porous support layer based on our experience because the porosity was gradually enhanced.

Pervaporation studies

A laboratory scale pervaporation system was used and the details of the apparatus have been described elsewhere.[25,39] An aqueous IPA solution with a water concentration of about 15 wt % was used as the feed solution and the operational temperature was 50°C. The feed circulation rate was kept at 0.5 l/min for each module. The permeate pressure was maintained less than 1 m bar by a vacuum pump. Retentate and permeate samples were collected at certain time interval after the membrane being conditioned for about 1.5 h.

Two apparent parameters, flux (J) and separation factor (α), were used for evaluating the pervaporation performance. The flux was determined by the permeate mass (Q) divided by the product of membrane area (A) and interval time (t)

$$J = \frac{Q}{At} \tag{3}$$

The separation factor was defined by the following equation

$$\alpha = \frac{Y_{w,i}}{Y_{w,j}} \times \frac{X_{w,j}}{X_{w,i}} \tag{4}$$

where Y_W and X_W are the weight fractions of components in the permeate and feed, respectively. Subscripts i and j refer to water and alcohol, respectively. The feed and permeate were analyzed through a Hewlett-Packard GC 6890 with a

Table 3. Fibers'ID and Their Corresponding Spinning Conditions

Fiber series	Outer layer polymer composition (wt/wt)	Outer layer dope concentration (wt%)	Coagulation temperature	Dope flow rate (ml/min)	Fiber ID
s/PPSU-30-AT	sPPSU/PPSU (50/50)	30	Ambient temperature	0.1	s/PPSU-30-AT-#1
s/PPSU-32-AT	sPPSU/PPSU (50/50)	32	Ambient temperature	0.1	s/PPSU-32-AT-#1
				0.1	s/PPSU-32-10-#1
				0.2	s/PPSU-32-10-#2
s/PPSU-32-10	sPPSU/PPSU (50/50)	32	10°C	0.3	s/PPSU-32-10-#3
				0.5	s/PPSU-32-10-#4
				0.7	s/PPSU-32-10-#5
sPPSU-32-10	sPPSU	32	10°C	0.1	sPPSU-32-10-#1
PPSU-32-10	PPSU	32	10^{0}C	0.1	PPSU-32-10-#1

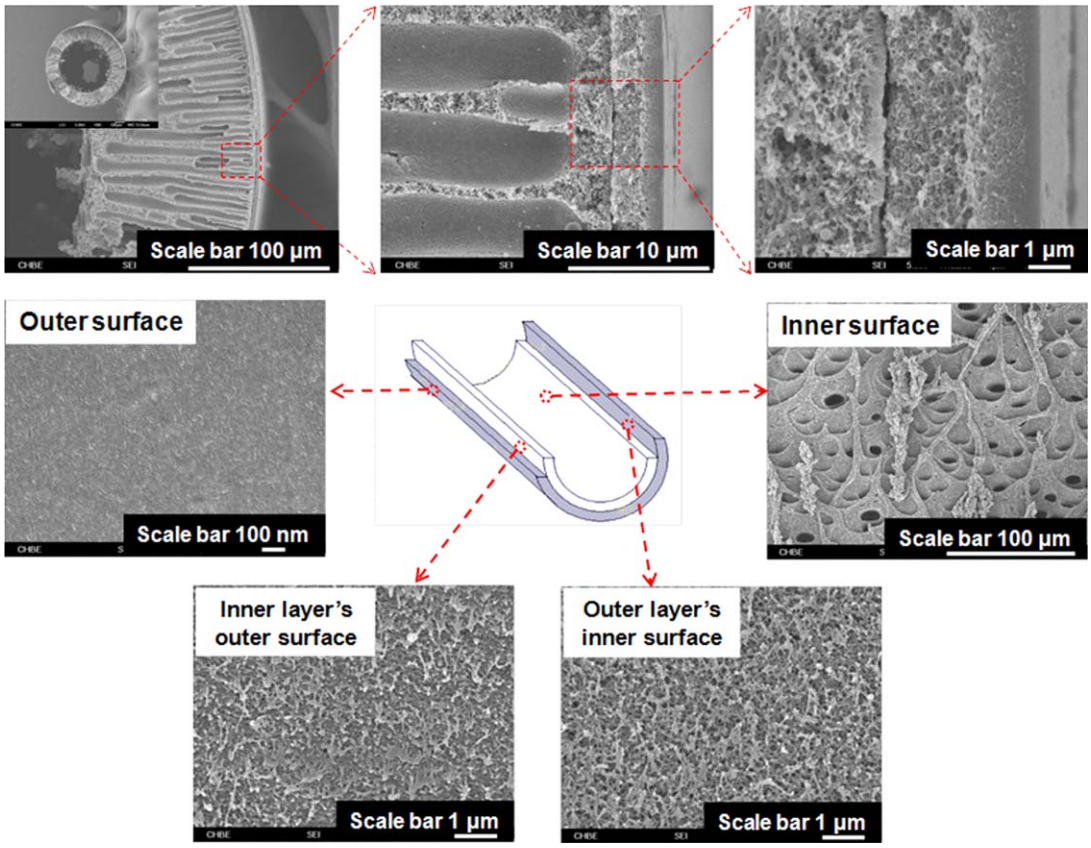

Figure 3. Morphology of a representative sPPSU/PPSU-based dual-layer hollow fiber membrane (ID: s/PPSU-32-10-#1).

[Color figure can be viewed in the online issue, which is available at wileyonlinelibrary.com.]

HP-INNOWAX column (packed with cross-linked polyethylene glycol) and a thermal conductivity detector (TCD).

Results and Discussion

Morphology study of the as-spun dual-layer hollow fiber membranes

Figure 3 represents a typical SEM morphology of the dual-layer hollow fiber membrane (ID: s/PPSU-32-10-#1). The cross-section images show a porous finger-like structure at the inner layer and an asymmetric structure at the outer layer, which are desirable for the pervaporation process. The finger-like structure of the inner layer does not contribute substantial transport resistance and, thus, promote the permeation flux. The asymmetric structure of the outer layer consists of a dense outer edge and a sponge-like porous inner edge. In other words, the dual-layer hollow fiber membrane visually presents a three layer structure, that is, a dense skin layer, a sponge-like porous layer, and a finger-like porous layer. Surface and interface morphology were further examined to evaluate their potential for pervaporation. As shown in Figure 3, a dense outer surface can be observed at a high magnification (×100,000), which is a prerequisite for achieving high separation efficiency in the pervaporation process. The inner surface is fully porous due to the delayed demixing process. The interface, including both the outer layer's inner surface and the inner layer's outer surface, also displays a microporous structure, which is in favor of high productivity.

The interfacial morphology is a unique feature in dual-layer hollow fiber membranes. A seamless interface is favorable in terms of fiber integrity, which is to the benefit of antiswelling property and mechanical stability. It mainly depends on the miscibility and concentration difference of inner- and outer-layer dopes. If the polymers, solvents, and additives used in both dopes are thermodynamically compatible, mutual diffusion may occur during phase inversion because of chemical potential differences, thus a seamless interface would be obtained. In addition, spinning parameters, such as dope flow ratio, air gap, and so on, may also affect the interfacial morphology. The interfacial morphology of s/PPSU-32-10-#1 in Figure 3 indicates that no obvious delamination can be observed at the interface but a boundary

Table 4. Pervaporation Performance of sPPSU/PPSU Based Hollow Fiber Membranes Spun with Different Outer Layer Concentration

Fiber ID	Outer layer dope concentration (wt%)	H_2O conc. in feed (wt%)	Flux (kg/m^2-h)	H_2O conc. in permeate (wt%)	Separation factor α
s/PPSU-30-AT-#1	30	14.27	4.83	91.59	65.37
s/PPSU-32-AT-#1	32	14.44	3.80	92.89	77.45

Table 5. Pervaporation Performance of sPPSU/PPSU Based Hollow Fiber Membranes Spun at Different Coagulation Temperature

Fiber ID	Coagulation temperature (°C)	H_2O conc. in feed (wt%)	Flux (kg/m^2-h)	H_2O conc. in permeate (wt%)	Separation factor α
s/PPSU-32-AT-#1	Ambient temperature	14.44	3.80	92.89	77.45
s/PPSU-32-10-#1	10	13.94	3.47	96.19	155.86

between them can be clearly recognized. The nondelaminated interface is attributed to the good compatibility between PPSU and sPPSU because they comprise the same main-chain structure that promotes mutual diffusion between these two layers. However, two other factors may retard the mutual diffusion: (1) the ethylene glycol additive in the inner layer because it may reduce their compatibility and (2) the difference in shrinkage rate between these two layers due to a large difference in dope concentration.

Pervaporation performance for IPA dehydration

Effect of Outer-Layer Dope Concentration. The physical and chemical properties of the outer-layer polymer dope play an important role to obtain dual-layer hollow fiber membranes with a favorable structure and separation performance for pervaporation. The dope concentration and composition of the outer layer will not only determine the quality of the dense-selective layer, but also affect the overall membrane integrity. A polymer concentration equal or higher than the critical concentration was normally selected to form a dense-selective skin for separations following the solution–diffusion mechanism.[22–27] This is due to the fact that a polymer dope at the critical polymer concentration or above shows a significant degree of chain entanglement that would produce hollow fibers with minimum defects.[40]

Based on viscosity curves in Figure 2, dope concentrations of 30 and 32 wt % were chosen to investigate the effect of dope concentration. Table 4 tabulates the pervaporation performance of fiber s/PPSU-30-AT-#1 and s/PPSU-32-AT-#1. It can be observed that the flux drops significantly from 4.83 to 3.80 kg/m^2h, while the separation factor slightly increases as the outer-layer dope concentration increases by 2 wt %. Comparing to the separation performance of our previous work,[3] one may note that both dense-selective layers are not defect-free probably due to the slow phase inversion process. In addition, the flux was significantly sacrificed by increasing dope concentration, indicating that it may not be preferable to improve separation factor by further increasing dope

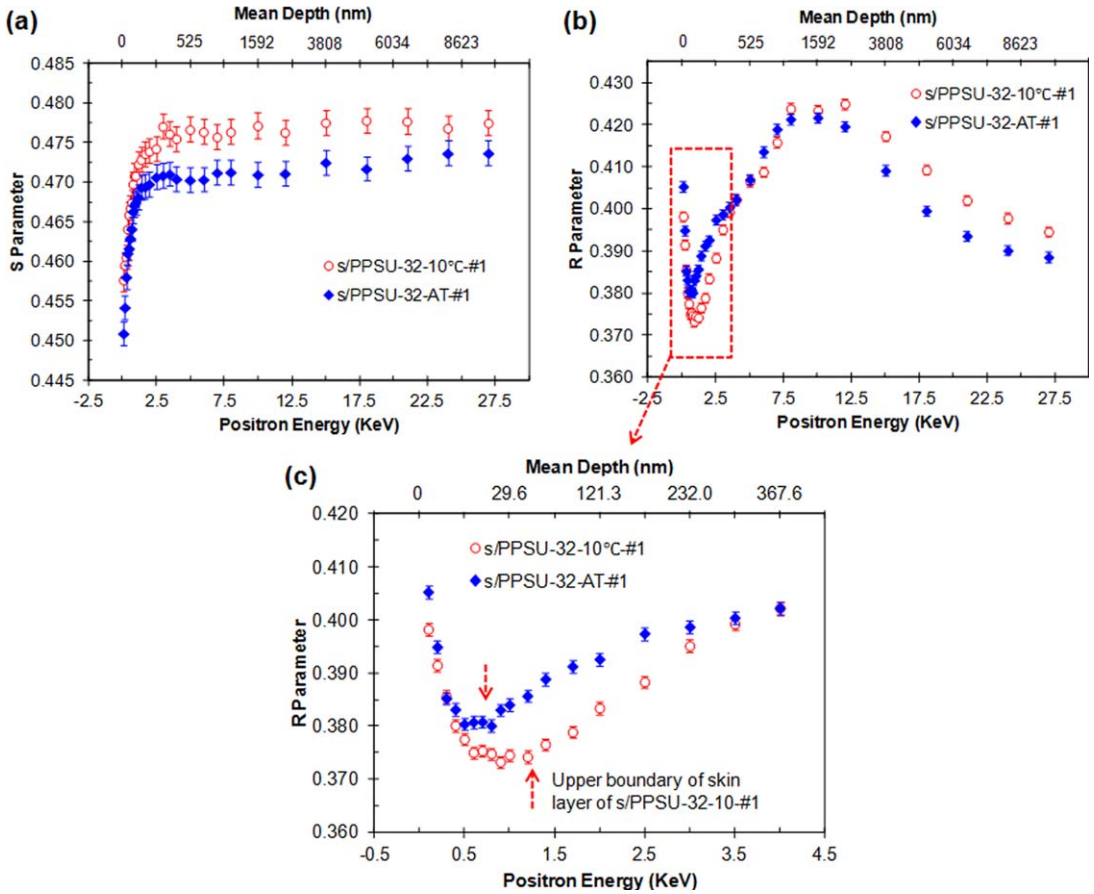

Figure 4. S and R parameters for sPPSU/PPSU based hollow fiber membranes spun at different coagulation temperature as a function of incident positron energy (or mean depth).

[Color figure can be viewed in the online issue, which is available at wileyonlinelibrary.com.]

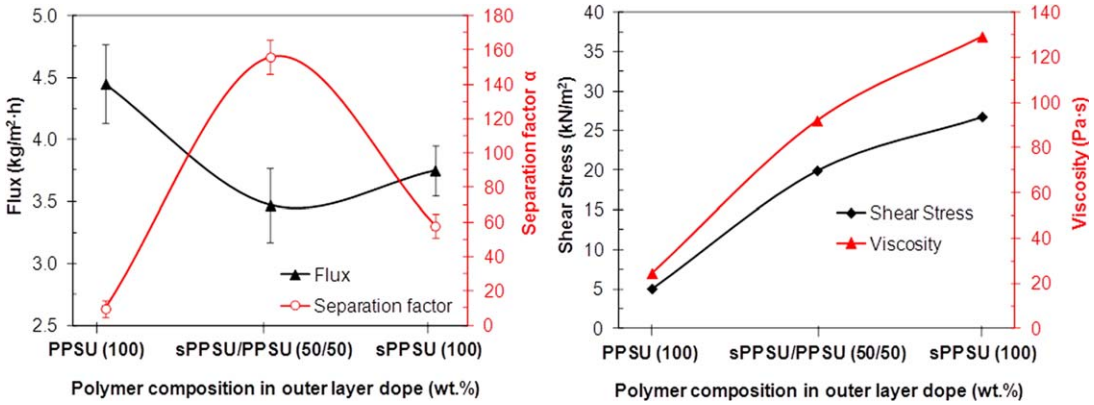

Figure 5. Pervaporation performance of sPPSU/PPSU based hollow fiber membranes spun with different outer layer polymer compositions and their corresponding dope viscosities and shear stress at the outer edge.

[Color figure can be viewed in the online issue, which is available at wileyonlinelibrary.com.]

concentration. Efforts should be taken to overcome this trade-off among flux, separation factor, and dope concentration by adjusting other spinning parameters.

Effect of Coagulation Temperature. The use of hydrophilic materials such as sPPSU polymer is highly desirable to facilitate water transport across the membrane. However, hydrophilic materials typically induce delayed demixing and results in a less perfect skin layer with a low separation factor. Therefore, it is necessary to tailor the spinning parameters to overcome this problem. One of the ways to accelerate the demixing process is to lower coagulation temperature during spinning because it may provide the following effects:[39,41,42] (1) changing the basic phase diagram, (2) inducing vigorous skin formation, and (3) expediting the precipitation of the outer surface during phase inversion. A new batch of dual-layer hollow fiber membranes comprising a 50/50 (wt/wt) sPPSU/PPSU in the outer-layer dope was, therefore, spun at a coagulation temperature of 10°C (ID: s/PPSU-32-10 series). Table 5 displays its separation performance. As can be observed, s/PPSU-32-10-#1 shows a slightly lower flux but a double separation factor compared to that spun at ambient temperature (ID: s/PPSU-32-AT-#1). Clearly, decreasing coagulation temperature may be a more effective and direct way than increasing dope concentration to spin hydrophilic polymers with improved separation factor but without much sacrificing flux.

Figure 4 shows the depth profiles of s/PPSU-32-10-#1 and s/PPSU-32-AT-#1 dual-layer hollow fiber membranes as a function of incident positron energy by PAS. The Doppler-broadened line-width in DBES spectra are typically described by two parameters: S and R parameters.[35,36] S parameter, derived from 2γ annihilation in DBES spectra, measures the free volumes with a size less than 1 nm.[35] There are three main factors contributing to the S parameter in polymers: (1) free-volume content (based on para-Positronium (p-Ps) annihilation), (2) free-volume size (based on the uncertainty principle), and (3) chemical composition. R parameter measures the relative amount of 3γ annihilation, which could be contributed from o-Ps in vacuum or in large pores. It provides information about the existence of large pores (nm–μm).[35]

As shown in Figure 4a, the S parameter near the top membrane surface increases rapidly to a maximum and then turns to a plateau with an increase in incident positron energy. This is a typical trend for polymeric membranes. The sharp ramp at the low positron energy range, which correspond to the membrane surface and near surface, is probably attributed to the back diffusion and scattering of positronium.[35,37] The higher S parameter of s/PPSU-32-10-#1 at the plateau indicates either a larger free volume size or a higher free volume content in the dense skin layer of s/PPSU-32-10-#1 compared with s/PPSU-32-AT-#1. As a consequence, it can be deduced that the dense-selective skin of s/PPSU-32-10-#1 has a looser structure at molecular level and a higher intrinsic permeability than that of s/PPSU-32-AT-#1. This phenomenon is resulted from rapid quench and slow chain rearrangement at low coagulation temperature, which usually leads to a low density of chain packing.

The R parameter in Figure 4b shows a drastically descending trend from the outer membrane surface and then reaches a peak valley, which is identified as the dense skin layer. The sharp decrease of R parameter near the membrane surface may be also due to the back diffusion of positronium.[35,37] Figure 4c is an enlargement of R parameter at the positron energy range of 0–4.5 KeV. The following facts can be observed: (1) s/PPSU-32-10-#1 shows a lower R parameter at the peak valley than s/PPSU-32-AT-#1, indicating the former has a less defective skin layer and a slightly tighter substructure just beneath the dense layer than the latter because R parameter reflects the existence of big pores with sizes from nanometer to micrometer. (2) The width of the peak valley of s/PPSU-32-10-#1 is larger than that of s/PPSU-32-AT-#1, implying that s/PPSU-32-10-#1 has a thicker skin layer due to a rapider coagulation at a lower temperature. By fitting the R parameter curves with the aid of VEPFIT software, the thicknesses of the dense skin layer for s/PPSU-32-10-#1 and s/PPSU-32-AT-#1 are about 35 and 15 nm, respectively.

Both results from S and R parameters are consistent with the pervaporation performance shown in Table 5. The existence of a thicker dense skin layer with less defective pores in s/PPSU-32-10-#1 is the major driving force for the remarkable increment in separation factor. On the other hand, the relatively higher intrinsic permeability in the dense skin layer of s/PPSU-32-10-#1 provides a persistently high flux. As a result, even though the dense-layer thickness increases from 15 to 35 nm and there is a slightly tighter substructure just beneath the dense layer when lowering the coagulation

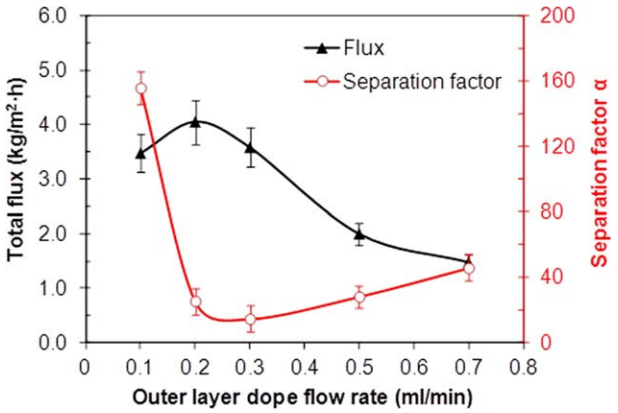

Figure 6. Pervaporation performance of s/PPSU-32-10 series hollow fiber membranes as a function of outer layer dope flow rate.

[Color figure can be viewed in the online issue, which is available at wileyonlinelibrary.com.]

temperature from ambient temperature to 10°C, only a minor flux decline is observed. The flux data also imply that the slightly tighter substructure just beneath the dense layer did not play an important role.

Effect of Outer-Layer Dope Composition. In addition to spinning s/PPSU-32-10 series of fibers that consist of 50/50 (wt/wt) sPPSU/PPSU in the outer layer as described in the previous section, we have spun two more batches of fibers with PPSU (ID: PPSU-32-10-#1) and sPPSU (ID: sPPSU-32-10-#1) as the outer layer, respectively, at 10°C to study the effects of the outer-layer dope composition on IPA dehydration. Figure 5 compares their separation performance. The separation factor follows an up-and-down trend while flux goes the opposite way as the hydrophilic sPPSU component increase in the outer layer.

In our previous work,[3] both flux and separation factor of dense flat membranes showed an uptrend as the degree of sulfonation increases. Apparently, separation performance of the hollow fiber membranes is not only a function of hydrophilicity/hydrophobicity of the dense-selective layer but also its perfectness. The perfectness of the dense-selective layer was determined by two engineering factors, namely, demixing rate and dope rheology. Since the demixing process of sPPSU is slow because of its hydrophilic nature, membrane spun from 100% sPPSU tends to have a loose dense skin. As a result, sPPSU-32-10-#1 fiber shows a high flux but an average separation factor. Apparently, s/PPSU-32-10-#1 fiber consisting of 50/50 sPPSU/PPSU in the outer layer has balanced hydrophilicity and demixing rate; thus, a tight dense-selective skin is formed with a higher separation factor but a slightly lower flux.

Second, the dope rheology including viscosity, shear, and elongational stresses during spinning may also play a critical role on the quality of the dense-selective layer. The dope solution experiences various stresses and relaxation when extruding through an annulus spinneret. For free fall spinning, these stresses may induce molecular orientation within the spinneret and relaxation such as die swell after exiting from the spinneret. As a result, they affect fiber's micromorphology, separation efficiency, and productivity. Since dope viscosity and shear stress within the spinneret increase with an increase in sPPSU content as shown in Figure 5, and a high shear stress tends to induce a thicker or higher oriented skin layer.[43–45] s/PPSU-32-10-#1 and sPPSU-32-10-#1 have higher separation factors than PPSU-32-10-#1. In addition, as shown in Table 1, dopes made from both sPPSU-32-10-#1 and s/PPSU-32-10-#1 display non-Newtonian fluid behavior, whereas the former has a higher viscosity than the latter. As a result, the former has a severer die swell than the latter. The die swell may interrupt the existing molecular orientation, induce microdefects in the dense-layer layer, and lower the separation performance of sPPSU-32-10-#1. Therefore, the separation factor shows an up-and-down trend with sPPSU content in the outer layer.

Effect of Outer-Layer Dope Flow Rate. Figure 6 shows the pervaporation performance of s/PPSU-32-10 series of hollow fiber membranes as a function of outer-layer dope flow rate from 0.1 to 0.7 ml/min. The flux increases slightly and then drops continuously, whereas the separation factor declines rapidly and then increases slowly. Figure 7 displays the evolution of cross section morphologies. The delamination phenomenon apparently occurs when the outer-layer dope flow rate increases from 0.1 to 0.2 and 0.3 ml/min (ID: s/PPSU-32-10-#2 and #3), but it gradually disappears when the outer-layer dope flow rate further increases to 0.4 and 0.5 ml/min (ID: s/PPSU-32-10-#4 and #5). These interesting phenomena are consistent with our hypotheses on the effect of die swell in the previous section.

As illustrated in Figure 8, there are four regions during hollow fiber spinning:[46] (1) shear flow region within the spinneret, (2) die swell region for flow rearrangement, (3) drawing, and (4) solidification regions. During die swell, the shear oriented polymer chains relax and rearrange back to a random coil structure. As a result, the outer-layer dope expands outward and also possibly inward into the inner-layer dope depending on (1) the degree of die swelling, (2) the compatibility of the two dopes, and (3) the speed of phase inversion. When the outer-layer dope flow rate is low (i.e., 0.1 ml/min), the phase inversion of this layer is fast that may minimize die swell so that both chain relaxation and inward diffusion occur hardly. Thus, the resultant membrane (ID: s/PPSU-32-10-#1) has the highest separation factor and a clear interface between the inner and outer layers. As the outer-layer flow rate increases, a severer die swell occurs that not only destroys or rearranges the existing skin orientation but also induces delamination from the inner layer. Consequently, the separation factors of s/PPSU-32-10-#2 and #3 drop rapidly due to defects formation or reduced chain orientation. If we further increase the outer-layer dope flow rate, it would delay the phase inversion, enhance mutual diffusion between the inner and outer layers and, thus, form an almost seamless interface as shown for the s/PPSU-32-10-#5 fiber in Figure 7 at a high magnification. On the other hand, macrovoids in the outer layer gradually appear with increasing outer-layer dope flow rate. This is probably due to the fact that a thicker unoriented outer layer is more vulnerable to the intrusion of the external coagulant.[47]

To confirm our hypotheses, s/PPSU-32-10-#1, #2, and #5 samples were selected to be analyzed by PAS since s/PPSU-32-10-#2 and #3 show comparable morphology and performance, so do s/PPSU-32-1-#4 and #5. Based on the depth profiles of S and R parameters, Figure 9 reveals that the dense layer thickness and the degree of densification follow the order of s/PPSU-32-10-#1 > s/PPSU-32-10-#5 > s/PPSU-32-10-#2. In other words, s/PPSU-32-10-#1 has a thick and more perfect dense layer; s/PPSU-32-10-#5 has a medium thick and less perfect dense layer, whereas s/PPSU-32-10-#2

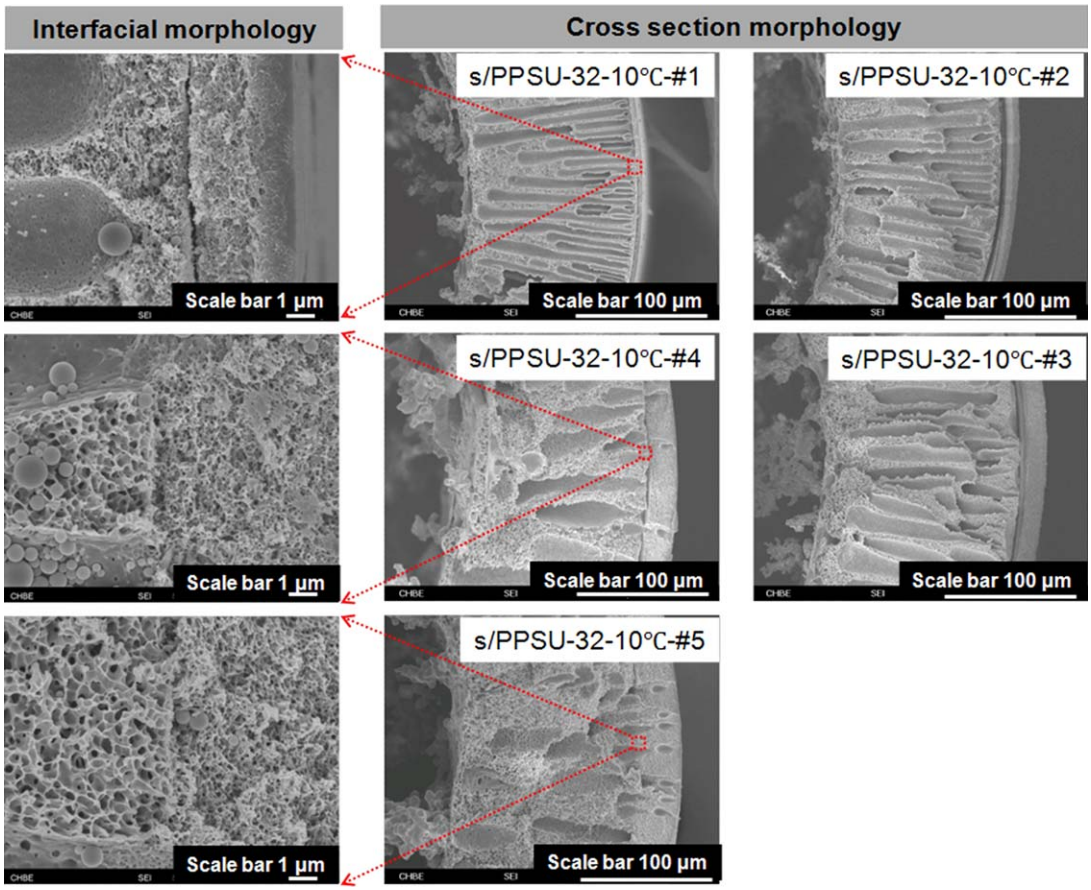

Figure 7. Cross-section morphology of s/PPSU-32-10 series dual-layer hollow fiber membranes.

[Color figure can be viewed in the online issue, which is available at wileyonlinelibrary.com.]

has a thin and more defective dense layer. Interestingly, these PAS results are well coherent with the trend of separation factor as shown in Figure 6.

Post thermal treatment of as-spun dual-layer hollow fiber membranes

Annealing has been frequently used to improve the separation efficiency of hollow fiber membranes. Usually, annealing can (1) promote thermal motion and release residual stresses of polymer chains, (2) repack polymer nodules, (3) densify skin layer, and (4) eliminate microdefects.[5,22,24–26,39,48] As a result, the thermally treated membrane may have a smaller free volume and a higher substructure resistance. Figure 10 shows the effects of thermal treatment at 150°C for 2 h on separation performance of s/PPSU-32-10-#1 dual-layer hollow fiber membranes. As expected, flux decreases while separation factor dramatically increases after thermal treatment. Figure 11 compares the cross-section morphology of s/PPSU-32-10-#1 membrane before and after thermal treatment. At a low magnification of 20,000, the cross-sections do not differ much visibly. But they are different from each other at a high magnification of 50,000. The thermally annealed fiber shows relatively more packed polymer nodules underneath the outer skin layer compared to the pristine fiber. The PAS results shown in Figure 12 further confirm the SEM observation and the trend of pervaporation performance. Specifically, the S value at the plateau becomes smaller after thermal treatment compared to the pristine hollow fiber membrane, indicating that the skin layer turns into denser during thermal annealing. The R parameter also indicates that the skin layer becomes denser and thicker after thermal treatment. The thicknesses of dense

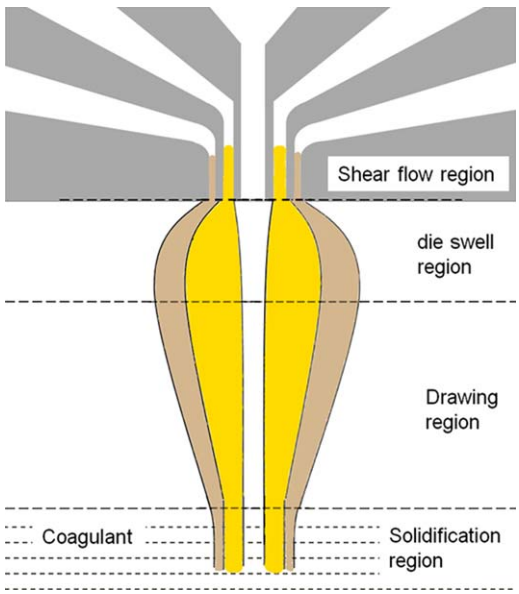

Figure 8. Hollow fiber spinning regions from Su et al.'s work.[46]

[Color figure can be viewed in the online issue, which is available at wileyonlinelibrary.com.]

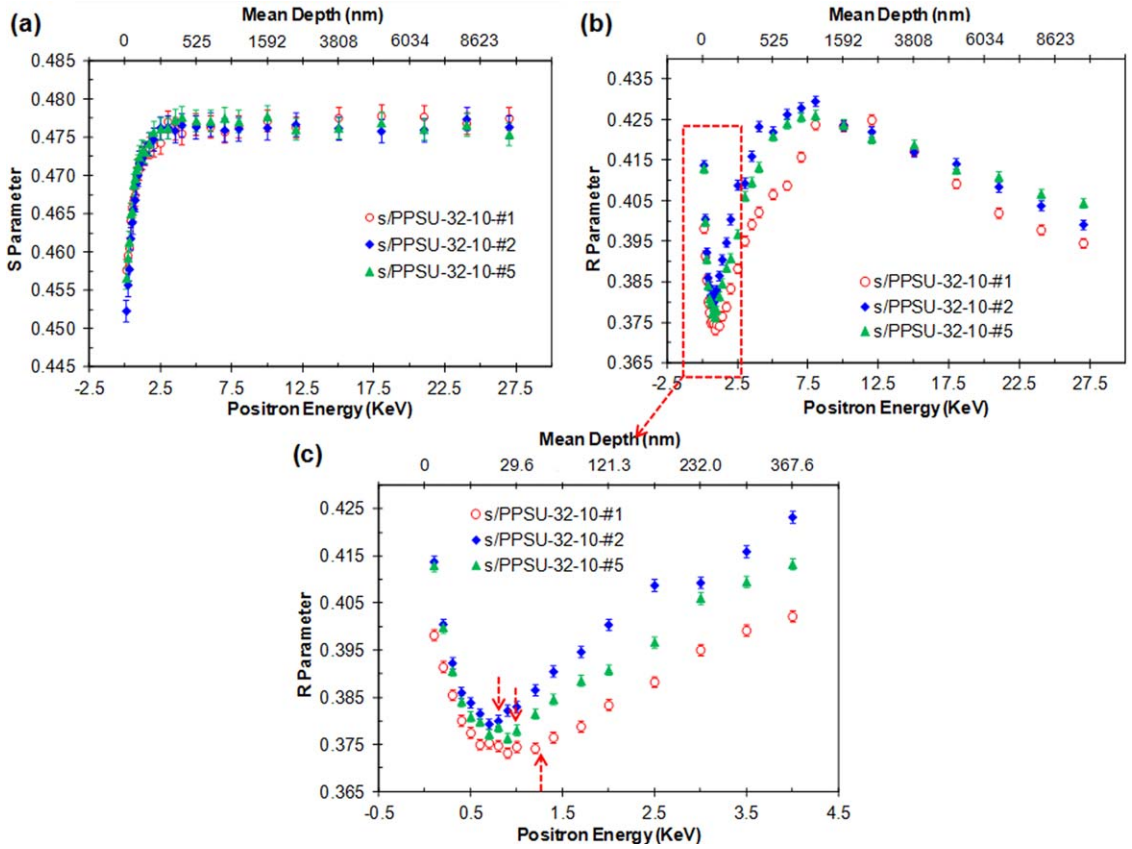

Figure 9. S and R parameters for sPPSU/PPSU based hollow fiber membranes spun with different outer layer dope flow rate (ID: sPPSU-32-10-#1, #2, and #5) as a function of incident positron energy (or mean depth).

[Color figure can be viewed in the online issue, which is available at wileyonlinelibrary.com.]

skin layers before and after thermal treatment for s/PPSU-32-10-#1 fiber are about 35 and 90 nm, respectively. Therefore, the separation factor of the annealed fiber was improved significantly with a compromised flux. However, the flux did not decline dramatically after thermal annealing. This may be attributed to the rearrangement of sulfonate groups in the dense-selective layer. Sulfonate groups can form hydrogen bonding with each other and water. During thermal annealing, the hydrophilic sulfonate groups, driven by electrostatic interaction, tend to agglomerate and form special channels for water transport as proposed by Shao and Huang.[49] Therefore, the facilitated water transportation by sulfonate groups may prevent the flux from dropping significantly.

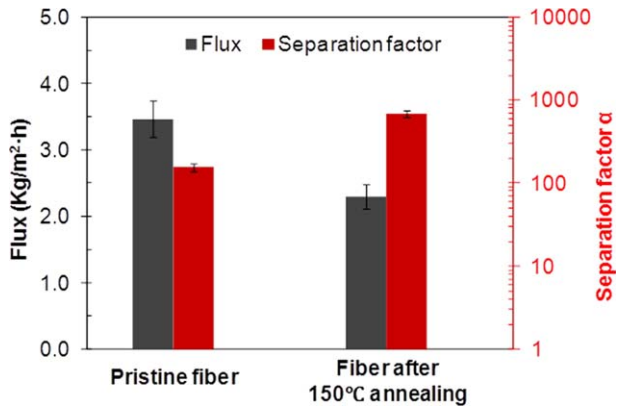

Figure 10. Effects of thermal treatment on separation performance of s/PPSU-32-10-#1 hollow fiber membrane.

[Color figure can be viewed in the online issue, which is available at wileyonlinelibrary.com.]

Benchmarking on pervaporation performance for IPA dehydration

Because of importance of IPA recycle, pervaporation dehydration of IPA has been studied by various materials. Tables 6 and 7 tabulate some of literature studies on dehydration of IPA in terms of materials and fabrication techniques,[7–11,13–19,22,26–32,39,48,50–55] whereas Figure 13 shows a graphical comparison of separation performance among different membranes. As can be observed, inorganic membranes[28–32] have superior pervaporation performance to polymeric membranes due to their high thermal stability and antiswelling properties. However, inorganic membranes are expensive. Their fragileness and poor processability also restrain their broad applications. Mixed matrix membranes were, therefore, proposed to cut down fabrication cost and to improve processability,[7–11,50] but so far their separation performance is generally below the expectation due to chain rigidification and partial pore blockage.[50] Polymeric composite membranes fabricated by LBL[13–16] and IP[17–19] techniques are also included for comparison. As shown in Figure 13, the sPPSU/PPSU-based membranes have impressive fluxes that are better than most polymeric membranes, surpassing those membranes made by LBL and IP, and approaching

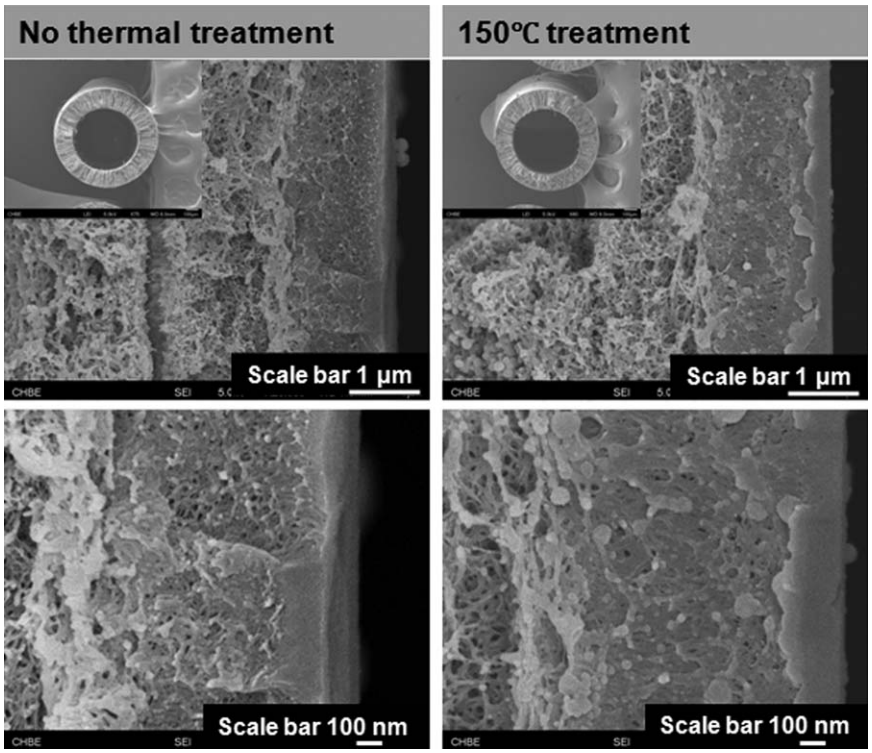

Figure 11. Cross-section morphology of s/PPSU-32-10-#1 hollow fiber membrane before and after thermal treatment at 150°C for 2 h.

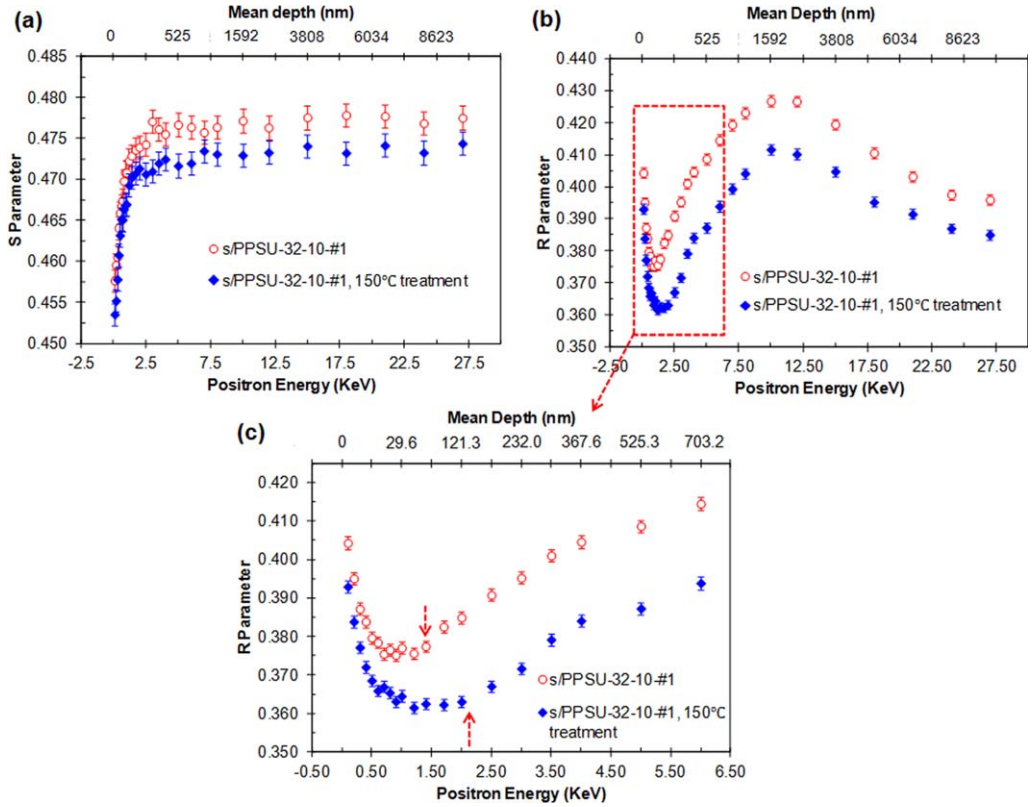

Figure 12. S and R parameters for s/PPSU-32-10-#1 hollow fiber membrane before and after thermal treatment as a function of incident positron energy (or mean depth).

[Color figure can be viewed in the online issue, which is available at wileyonlinelibrary.com.]

Table 6. Literature Data on Separation Performance for IPA Dehydration Various Membranes

Membrane	Temperature (/°C)	H_2O concn. in feed (wt%)	Flux (kg/m^2·h)	Separation factor α	Ref.
Inorganic membranes					
Zeolite T membranes	75	10	2.2	8,900	28
CHA-type zeolite membranes	75	10	2.93	1,800	29
Mordenite/ZSM-5 hybrid membrane	75	10	4.8	3,200	30
Micro-porous SiO_2-ZrO_2 membrane	75	10	2.16	15,000	31
Porous silica-zirconia membrane	75	10	9	1,500	32
Mixed matrix membranes (MMMs)					
Polyimide (BAPP-BODA)/zeolite 13X	25	10	0.15	272.3	7
P84 co-polyimide/Zeolite	60	15	0.1	1,000	8
PBI/ZIF-8	60	15	0.25	310	9
Matrimid/cyclodextrin	22.4	14	0.08	3,000	10
Matrimid/MgO	100	18	0.1	1,100	11
Layer-by-layer assembly (LBL)					
Oly(ethylenimine)/alginic acid	50	12	0.3	10,000	13
PVA/PVSu	58.5	10	1.7	990	14
PDDA)/PSS (10.5 bilayers)	50	10	1.8	315	15
PEC+/PDMC-CMCNa PEC$^-$ (24 bilayers)	50	10	1.18	1,013	16
PEC+/PDMC-CMCNa PEC$^-$ (25 bilayers)	50	10	1.36	938	
Interfacial Polymerization (IP)					
TETA-TMC/mPAN TFC membrane	25	30	1.3	736.5	17
MPDASA-TMC/mPAN TFC membrane	25	30	1.67	775.4	18
MPD-TMC/Torlon TFC hollow fiber	50	15	1.28	624	19

ceramic membranes, while their separation factors are reasonably high, comparable to those membranes made by LBL and IP, but still inherently poorer than ceramic membranes.

Table 7 also compares the current work with literature data on polymeric hollow fiber membranes for IPA dehydration.[22,26,27,39,48,51–55] Since it is not easy to fabricate a hollow fiber membrane with an ultrathin and defect-free skin layer, and it is difficult to overcome the swelling issue, most polymeric hollow fiber membranes do not possess both high flux and high separation factor simultaneously as shown in Figure 13. As a result, the sPPSU/PPSU-based dual-layer hollow fiber membranes display much better separation performance than most other polymeric hollow fiber membranes. Clearly, the remarkable separation properties are attributed to (1) the distinctive antiswelling resistance of the PPSU and sPPSU polymers and (2) synergistic combination

Table 7. Literature Data on Separation Performance for IPA Dehydration by Polymeric Hollow Fiber Membranes

Membrane	Post treatment	Temp. (/°c)	H_2O concn. in feed (wt%)	Flux (kg/m^2·h)	Separation factor α	Ref.
P84 co-polyimide/ polyethersulfone dual layer hollow fiber	NO	60	15	1.36	43.7	22
	Thermal treatment at 300°C for 1 h	60	15	0.60	125	
	Crosslinked by p-xylenediamine	60	15	0.45	950	
PAI/PEI dual-layer hollow fiber	Thermal treated at 75 °C, 2 h	60	15	0.77	1944	26
6FDA-ODA-NDA/Ultem® dual-layer hollow fiber	No	60	15	0.47	2516	27
P84 co-polyimide single layer hollow fiber	No	60	15	1.62	78	39
	Thermal treatment at 300°C for 1 h	60	15	0.88	10585	
PEG-added PAN single layer hollow fiber	20% PEG 200 addictive, heat - treated at 120 °C, 12 h	25	10	0.13	890	48
PVA-sodium alginate/PS composite hollow fiber	Crosslinked by maleic acid	45	15	0.75	1300	51
Matrimid® polyimide single layer hollow fiber	No	80	16	6.20	7.9	52
	Thermal treatment followed by Crosslinked by 1,3-propane diamine	80	16	1.8	132	
Chitosan/polysulfone composite hollow fiber	Surface modified by Sodium 4-styrenesulfonate	25	30	0.13	78	53
Carboxymethyl chitosan/polysulfone composite hollow fiber	Crosslinked by glutaraldehyde	45	12.5	0.39	3239	54
Torlon®/P84 co-polyamide-imide blended single layer hollow fiber	Crosslinked by p-xylenediamine	60	15	1.00	185	55
s/PPSU-30-AT-#1	Thermal treatment at 150 °C, 2 h	50	14.99	3.91	171.9	This work
s/PPSU-30-10°C-#1	No	50	13.94	3.47	155.9	This work
sPPSU/PPSU-30%-#1	Thermal treatment at 150 °C, 2 h	50	14.09	2.30	686.8	This work

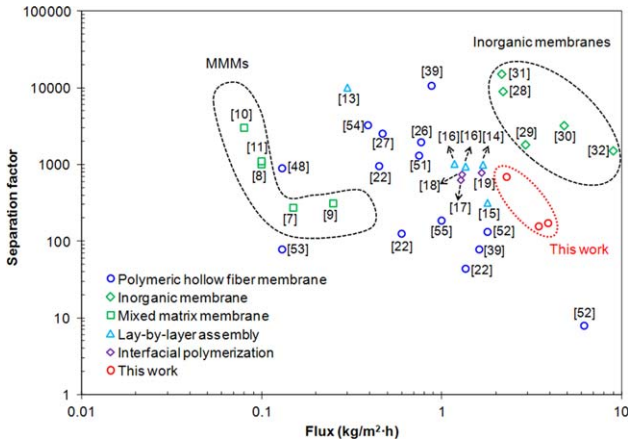

Figure 13. Graphical representation of the membrane performance for IPA dehydration.

[Color figure can be viewed in the online issue, which is available at wileyonlinelibrary.com.]

of these two polymers via molecular engineering of the dual-layer hollow fiber spinning process.

Conclusions

We have used the PPSU and sPPSU polymers to investigate the fundamental science and engineering to design dual-layer hollow fiber membranes with an ultrathin selective layer of 15–90 nm for the dehydration of IPA. By manipulating spinning conditions and analyzing by FESEM and PAS, the effects of dope composition and concentration, coagulation temperature and outer-layer dope flow rate on membrane morphology and pervaporation performance have been defined and harmoniously correlated. The following conclusions can be drawn from this work:

1. The sPPSU/PPSU-based dual-layer hollow fiber membranes display much better separation performance than most other polymeric hollow fiber membranes. The best performance of as-spun fibers was obtained from s/PPSU-32-10-#1 which was spun from a 16/16/68 wt % (sPPSU/PPSU/NMP) outer layer dope with an outer layer flow rate of 0.1 ml/min and coagulated at 10°C. The fiber has a dense-layer thickness of around 35 nm and shows a flux and separation factor of 3.47 kg/m^{2}h and 155.9, respectively.

2. The superior performance is attributed to the following factors: (1) the sulfonate groups of the outer-layer sPPSU polymer facilitate water transport across the membrane; (2) the inner-layer PPSU polymer provides antiswelling and operational stability; (3) the nondelamination structure between the inner and outer layers strengthens the fiber integrity; and (4) the nanometric thin dense-skin layer reduces mass transport resistance substantially.

3. Hydrophilic polymers have a slow phase inversion process. Dense-selective skins made of hydrophilic polymers tend to be loose. However, a high dope concentration can facilitate chain entanglement, a low coagulation temperature can induce a rapid quench, and a thermally annealing can remove defects and densify the selective skin. As a result, sPPSU/PPSU dual-layer hollow fibers with a much higher separation performance (i.e., a flux of 2.30 kg/m^{2}h and a separation factor of 686.8) can be formed by adjusting dope concentration, decreasing coagulation temperature and thermally annealing at 150°C for 2 h.

Acknowledgments

The authors would like to thank both BASF SE, Germany for the project "The Evaluation and Characterization of Ultrason® for Membrane Applications" (Grant number: R-279-000-283-597) and the Singapore National Research Foundation under its Competitive Research Program for the project entitled, "New Biotechnology for Processing Metropolitan Organic Wastes into Value-Added Products" (grant number: R-279-000-311-281) for funding this research. The authors would also like to thank Dr. P. Sukitpaneenit, Mr. Y. K. Ong, Ms. H. Wang, and other staffs in our lab for their help and suggestions on this work.

Literature Cited

1. Baker RW. Membrane Technology and Applications, 2nd ed. England: John Wiley &Sons Ltd, 2004.
2. Feng X, Huang RYM. Liquid separation by membrane pervaporation: a review. *Ind Eng Chem Res*. 1997;36:1048–1066.
3. Tang YP, Widjojo N, Shi GM, Chung TS, Weber M, Maletzko C. Development of flat–sheet membranes for C1–C4 alcohols dehydration via pervaporation from sulfonated polyphenylsulfone (sPPSU). *J Membr Sci*. 2012;415–416:686–695.
4. Shieh J-J, Huang RYM. Chitosan/N-methylol nylon 6 blend membranes for the pervaporation separation of ethanol-water mixtures. *J Membr Sci*. 1998;148:243–255.
5. Chung TS, Guo WF, Liu Y. Enhanced matrimid membranes for pervaporation by homogenous blends with polybenzimidazole (PBI). *J Membr Sci*. 2006;271:221–231.
6. Zereshki S, Figoli A, Madaeni SS, Simone S, Esmailinezhad M, Drioli E. Effect of polymer composition in PEEKWC/PVP blends on pervaporation separation of ethanol/cyclohexane mixture. *Sep Purif Technol*. 2010;75:257–265.
7. Li C-L, Huang S-H, Hung W-S, Kao S-T, Wang D-M, Jean YC, Lee K-R, Lai J-Y. Study on the influence of the free volume of hybrid membrane on pervaporation performance by positron annihilation spectroscopy. *J Membr Sci*. 2008;313:68–74.
8. Qiao X, Chung TS, Rajagopalan R. Zeolite filled P84 co-polyimide membranes for dehydration of isopropanol through pervaporation process. *Chem Eng Sci*. 2006;61:6816–6825.
9. Shi GM, Yang T, Chung TS. Polybenzimidazole (PBI)/zeolitic imidazolate frameworks (ZIF-8) mixed matrix membranes for pervaporation dehydration of alcohols. *J Membr Sci*. 2012;415–416:577–586.
10. Jiang LY, Chung TS. Homogeneous polyimide/cyclodextrin composite membranes for pervaporation dehydration of isopropanol. *J Membr Sci*. 2010;346:45–58.
11. Jiang LY, Chung TS, Rajagopalan R. Matrimid®/MgO mixed matrix membranes for pervaporation. *AIChE J*. 2007;53:1745–1757.
12. Bai J, Fouda AE, Matsuura T, Hazlett JD. A study on the preparation and performance of polydimethylsiloxane-coated polyetherimide membranes in pervaporation. *J Appl Polym Sci*. 1993;48:999–1008.
13. Meier-Haack J, Lenk W, Lehmann D, Lunkwitz K. Pervaporation separation of water/alcohol mixtures using composite membranes based on polyelectrolyte multilayer assemblies. *J Membr Sci*. 2001;184:233–243.
14. Toutianoush A, Tieke B. Pervaporation separation of alcohol/water mixtures using self-assembled polyelectrolyte multilayer membranes of high charge density. *Mater Sci Eng C*. 2002;22:459–463.
15. Yin M, Qian J, An Q, Zhao Q, Gui Z, Li J. Polyelectrolyte layer-by-layer self-assembly at vibration condition and the pervaporation performance of assembly multilayer films in dehydration of isopropanol. *J Membr Sci*. 2010;358:43–50.
16. Zhao Q, Qian J, An Q, Sun Z. Layer-by-layer self-assembly of polyelectrolyte complexes and their multilayer films for pervaporation dehydration of isopropanol. *J Membr Sci*. 2010;346:335–343.
17. Huang S-H, Hung W-S, Liaw D-J, Tsai H-A, Jiang GJ, Lee K-R, Lai J-Y. Positron annihilation study on thin-film composite pervaporation membranes: correlation between polyamide fine structure and different interfacial polymerization conditions. *Polymer*. 2010;51:1370–1376.
18. Kao S-T, Huang S-H, Liaw D-J, Chao W-C, Hu C-C, Li C-L, Wang D-M, Lee K-R, Lai J-Y. Interfacially polymerized thin-film

composite polyamide membrane: positron annihilation spectroscopic study, characterization and pervaporation performance. *Polym J*. 2010;42:242–248.
19. Zuo J, Wang Y, Sun SP, Chung TS. Molecular design of thin film composite (TFC) hollow fiber membranes for isopropanol dehydration via pervaporation. *J Membr Sci*. 2012;405–406:123–133.
20. Matsuyama H, Kariya A, Teramoto M. Characteristics of plasma polymerized membrane from octamethyltrisiloxane and its application to the pervaporation of ethanol-water mixture. *J Membr Sci*. 1994;88:85–92.
21. Li C-L, Tu C-Y, Inagaki N, Lee K-R, Lai J-Y. Plasma-induced solid-state polymerization modified poly(tetrafluoroethylene) membrane for pervaporation separation of aqueous alcohol mixtures. *J Appl Polym Sci*. 2006;102:909–919.
22. Liu RX, Qiao XY, Chung TS. Dual-layer P84/polyethersulfone hollow fibers for pervaporation dehydration of isopropanol. *J Membr Sci*. 2007;294:103–114.
23. Wang KY, Chung TS, Rajagopalan R. Dehydration of tetrafluoropropanol (TFP) by pervaporation via novel PBI/BTDA-TDI/MDI copolyimide (P84) dual-layer hollow fiber membranes. *J Membr Sci*. 2007;287:60–66.
24. Shi GM, Wang Y, Chung TS. Dual-layer PBI/P84 hollow fibers for pervaporation dehydration of acetone. *AIChE J*. 2012;58:1133–1145.
25. Jiang LY, Chen H, Jean Y-C, Chung TS. Ultrathin polymeric interpenetration network with separation performance approaching ceramic membranes for biofuel. *AIChE J*. 2009;55:75–86.
26. Wang Y, Goh SH, Chung TS, Na P. Polyamide-imide/polyetherimide dual-layer hollow fiber membranes for pervaporation dehydration of C1–C4 alcohols. *J Membr Sci*. 2009;326:222–233.
27. Widjojo N, Chung TS. Pervaporation dehydration of C2–C4 alcohols by 6FDA-ODA-NDA/Ultem® dual-layer hollow fiber membranes with enhanced separation performance and swelling resistance. *Chem Eng J*. 2009;155:736–743.
28. Asaeda M, Sakou Y, Yang J, Shimasaki K. Stability and performance of porous silica-zirconia composite membranes for pervaporation of aqueous organic solutions. *J Membr Sci*. 2002;209:163–175.
29. Cui Y, Kita H, Okamoto K-I. Zeolite T membrane: preparation, characterization, pervaporation of water/organic liquid mixtures and acid stability. *J Membr Sci*. 2004;236:17–27.
30. Yang J, Yoshioka T, Tsuru T, Asaeda M. Pervaporation characteristics of aqueous–organic solutions with microporous SiO_2–ZrO_2 membranes: experimental study on separation mechanism. *J Membr Sci*. 2006;284:205–213.
31. Li X, Kita H, Zhu H, Zhang Z, Tanaka K, Okamoto K-i. Influence of the hydrothermal synthetic parameters on the pervaporative separation performances of CHA-type zeolite membranes. *Microporous Mesoporous Mater*. 2011;143:270–276.
32. Sato K, Sugimoto K, Kyotani T, Shimotsuma N, Kurata T. Laminated mordenite/ZSM-5 hybrid membranes by one-step synthesis: preparation, membrane microstructure and pervaporation performance. *Microporous Mesoporous Mater*. 2012;160:85–96.
33. Lee YM, Nam SY, Ha SY. Pervaporation of water/isopropanol mixtures through polyaniline membranes doped with poly(acrylic acid). *J Membr Sci*. 1999;159:41–46.
34. Jean YC, Chen H, Zhang S, Chen H, Lee LJ, Awad S, Huang J, Lau CH, Wang H, Li F, Chung TS. Characterizing free volumes and layer structures in polymeric membranes using slow positron annihilation spectroscopy. *J Phys Conf Ser*. 2011;262:012027.
35. Chen H, Hung W-S, Lo C-H, Huang S-H, Cheng M-L, Liu G, Lee K-R, Lai J-Y, Sun Y-M, Hu C-C, Suzuki R, Ohdaira T, Oshima N, Jean YC. Free-volume depth profile of polymeric membranes studied by positron annihilation spectroscopy: layer structure from interfacial polymerization. *Macromolecules*. 2007;40:7542–7557.
36. Jean YC, Mallon PE, Schrader DM. Principles and Applications of Positron & Positronium Chemistry. Singapore: World Scientific Publishing Co. Pte. Ltd., 2003.
37. Li FY, Li Y, Chung TS, Chen H, Jean YC, Kawi S. Development and positron annihilation spectroscopy (PAS) characterization of polyamide imide (PAI)–polyethersulfone (PES) based defect-free dual-layer hollow fiber membranes with an ultrathin dense-selective layer for gas separation. *J Membr Sci*. 2011;378:541–550.
38. Chen GQ, Scholes CA, Doherty CM, Hill AJ, Qiao GG, Kentish SE. Modeling of the sorption and transport properties of water vapor in polyimide membranes. *J Membr Sci*. 2012;409–410:96–104.
39. Liu R, Qiao X, Chung TS. The development of high performance P84 co-polyimide hollow fibers for pervaporation dehydration of isopropanol. *Chem Eng Sci*. 2005;60:6674–6686.
40. Chung TS, Teoh SK, Hu X. Formation of ultrathin high-performance polyethersulfone hollow-fiber membranes. *J Membr Sci*. 1997;133:161–175.
41. Chung TS, Kafchinski ER. The effects of spinning conditions on asymmetric 6FDA/6FDAM polyimide hollow fibers for air separation. *J Appl Polym Sci*. 1997;65:1555–1569.
42. Jiang L, Chung TS, Li DF, Cao C, Kulprathipanja S. Fabrication of matrimid/polyethersulfone dual-layer hollow fiber membranes for gas separation. *J Membr Sci*. 2004;240:91–103.
43. Chung TS, Teoh SK, Lau WWY, Srinivasan MP. Effect of shear stress within the spinneret on hollow fiber membrane morphology and separation performance. *Ind Eng Chem Res*. 1998;37:3930–3938.
44. Qin J, Chung TS. Effect of dope flow rate on the morphology, separation performance, thermal and mechanical properties of ultrafiltration hollow fibre membranes. *J Membr Sci*. 1999;157:35–51.
45. Wang R, Chung TS. Determination of pore sizes and surface porosity and the effect of shear stress within a spinneret on asymmetric hollow fiber membranes. *J Membr Sci*. 2001;188:29–37.
46. Su Y, Lipscomb GG, Balasubramanian H, Lloyd DR. Observations of recirculation in the bore fluid during hollow fiber spinning. *AIChE J*. 2006;52:2072–2078.
47. Widjojo N, Chung TS. Thickness and air gap dependence of macrovoid evolution in phase-inversion asymmetric hollow fiber membranes. *Ind Eng Chem Res*. 2006;45:7618–7626.
48. Tsai H-A, Ma L-C, Yuan F, Lee K-R, Lai J-Y. Investigation of post-treatment effect on morphology and pervaporation performance of PEG added PAN hollow fiber membranes. *Desalination*. 2008;234:232–243.
49. Shao P, Huang RYM. Polymeric membrane pervaporation. *J Membr Sci*. 2007;287:162–179.
50. Chung TS, Jiang LY, Li Y, Kulprathipanja S. Mixed matrix membranes (MMMs) comprising organic polymers with dispersed inorganic fillers for gas separation. *Prog Polym Sci*. 2007;32:483–507.
51. Dong YQ, Zhang L, Shen JN, Song MY, Chen HL. Preparation of poly(vinyl alcohol)-sodium alginate hollow-fiber composite membranes and pervaporation dehydration characterization of aqueous alcohol mixtures. *Desalination*. 2006;193:202–210.
52. Jiang LY, Chung TS, Rajagopalan R. Dehydration of alcohols by pervaporation through polyimide asymmetric hollow fibers with various modifications. *Chem Eng Sci*. 2008;63:204–216.
53. Liu Y-L, Yu C-H, Ma L-C, Lin G-C, Tsai H-A, Lai J-Y. The effects of surface modifications on preparation and pervaporation dehydration performance of chitosan/polysulfone composite hollow-fiber membranes. *J Membr Sci*. 2008;311:243–250.
54. Shen J-N, Wu L-G, Qiu J-H, Gao C-J. Pervaporation separation of water/isopropanol mixtures through crosslinked carboxymethyl chitosan/polysulfone hollow-fiber composite membranes. *J Appl Polym Sci*. 2007;103:1959–1965.
55. Teoh MM, Chung TS, Wang KY, Guiver MD. Exploring torlon/P84 co-polyamide-imide blended hollow fibers and their chemical crosslinking modifications for pervaporation dehydration of isopropanol. *Sep Purif Technol*. 2008;61:404–413.

Manuscript received Dec. 21, 2012, and revision received Feb. 6, 2013.